Evolutionary approaches for surgical path planning: a quantitative study on Deep Brain Stimulation

Noura Hamze
Universität Innsbruck
Technikerstraße, 21A
6020 Innsbruck, Austria
noura.hamze@uibk.ac.at

Pierre Collet
ICube, Université de Strasbourg
300, bd. Sébastien Brant
67412 Illkirch, France
collet@unistra.fr

Caroline Essert
ICube, Université de Strasbourg
300, bd. Sébastien Brant
67412 Illkirch, France
essert@unistra.fr

***Abstract*—Path planning for surgical tools in minimally invasive surgery is a multi-objective optimization problem consisting in searching the best compromise between multiple placement constraints to find an optimal insertion point for the tool. Many works have been proposed to automate the decision-making process. Most of them use an aggregative approach that transforms the problem into a mono-objective problem. However, despite its intuitiveness, this approach is known for its incapacity to find all optimal solutions. After a previous clinical study in which we pointed out the interest of introducing MOEAs to neurosurgery [12], in this work, we aim at maximizing the range of optimal solutions proposed to the surgeon. Our study compares three different optimization approaches: an aggregative method using a weighted sum of the multiple constraints, an evolutionary multi-objective method, and an exhaustive dominance-based method used as ground truth. For each approach, we extract the set of all optimal insertion points based on dominance rules, and analyze the common and differing solutions by comparing the surfaces they cover. The experiments have been performed on 30 images datasets from patients who underwent a Deep Brain Stimulation electrode implant in the brain. It can be observed that the areas covered by the optimal insertion points obtained by the three methods differ significantly. The obtained results show that the traditional weighted sum approach is not sufficient to find the totality of the optimal solutions. The Parteo-based approaches provide extra solutions, but neither of them could find the complete optimal solution space. Further works should investigate either hybrid or extended methods such as adaptive weighted sum, or hybrid visualization of the solutions in the GUI.**

I. Introduction

Image-guided surgery has become very common in hospitals nowadays. It has many advantages compared to open surgery such as less skin and tissue trauma, less bleeding, less scarring, and faster recovery with shorter hospital stay. However, its major difficulties are the reduced visibility inside the patient's body, and the limited maneuvering of surgical tools. Therefore, an efficient preoperative planning is a key element of its success. More particularly, planning a safe and efficient trajectory for a surgical tool on preoperative medical images is a crucial and a challenging task which requires a long experience. The path is usually chosen as the best compromise between multiple surgical rules that can often be contradictory such as for instance: accurate targeting, avoidance of vessels or other sensitive structures, compliance with standards, short path, etc.

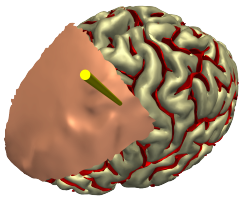

Fig. 1: Deep Brain Stimulation

Most of the automatic trajectory planning techniques that have been proposed in the literature in the past years are based on mono-objective optimization approaches. They combine all the surgical rules in a single aggregative cost function, after assigning certain importance weights, and minimize it to find an optimal solution strategy. This approach is intuitive, and sounds close to the current decision making process. However, the optimization community has shown that using mono-criteria approaches for solving multi-criteria optimization problems through aggregation of criteria can lead to an under-detection of the optimal solutions in a given solution space.

The purpose of this work is to better clarify and quantify the impact of the capacity and limits of different optimization approaches on the particular case of surgical trajectory planning. We investigate three optimization approaches: an aggregative method based on a weighted sum, an evolutionary dominance based approach and a random search method with dominance selection. We confront them on a use-case consisting of planning an optimal trajectory for electrodes paths in Deep Brain Stimulation (DBS), which is a neurosurgical treatment destined to treat the movement disorders such as Parkinson's disease or essential tremors (illustration on Fig. 1). For each method, we compute Pareto fronts among candidate entry points, and analyze the surfaces covered by the optimal solutions.

After reporting the closest works in Section II, we explain in Section III the three approaches implemented in our work. In Section IV, we describe the experimental setup. In Section V we conclude the paper detailing the results and discussing them, and compare the different methods.

978-1-5090-4601-0/17/$31.00

II. Related works

The resolution of multiple placement rules for automatic preoperative path planning of surgical tools has already been addressed by many groups. However, most of the works in the literature have adopted aggregative methods to solve this multi-objective problem. For instance, authors of [2], [3], [8], [11], [21] have all used a weighted sum to solve DBS electrode placement, while authors of [1], [18] also used a weighted sum to solve needle placement for needle placement in the liver for instance for radiofrequency ablation (RFA) of hepatic tumors. The choice of the weighted sum method seems intuitive, as surgeons usually have a reasonable idea of priorities between the rules and this approach enables to associate weights to priorities and get the corresponding solution instantly. However, this approach has some well-known drawbacks that are well explained in [6], [14]: the optimal solution distribution is often not uniform, and many optimal solutions cannot be detected in non-convex regions.

If multi-criteria methods are already widely used for radiation therapy planning [4], it's only recently that a very small number of groups have started to consider techniques based on Pareto-optimality to solve multiple criteria for trajectory planning in minimally invasive surgery. For example, a non-dominance based optimization has been used in [19], [20] to find a compromise between multiple clinical criteria for access paths in RFA. The result of the planning has been represented as a set of a few Pareto-optimal points that the surgeon could select to have information on how they satisfy each rule. So far, in this application field this kind of approach appears less intuitive for the user who has to browse the solution space. To our knowledge, multi-criteria approaches have not been investigated for neurosurgical trajectory planning.

Even if the differences between multi-objective and aggregative optimization methods are known, we wanted to measure their impact and compare their extent over the surface of candidate insertion points.

III. Materials and Methods

In this section we introduce some basic definitions and explain the three optimization approaches used in this study.

Strict dominance. We define dom the strict dominance relationship between two individuals x and y of the solution space $\mathcal{S}$ for a set of n objective functions f_i as follows:

$$\begin{array}{c} \forall \quad x, y \in \mathcal{S} \\ x \quad dom \quad y \quad \Longleftrightarrow \forall i \in [1..n] \quad , \quad f_i(x) < f_i(y) \end{array}$$

Pareto-optimal solution. A solution x is Pareto-optimal if it is not dominated by any other solution in the solution space $\mathcal{S}$.

$$\begin{array}{c} x \in \mathcal{S} \quad \text{is } \textit{Pareto} \text{ optimal} \\ \Longleftrightarrow \quad \forall \quad y \in \mathcal{S} \quad , \quad \neg(y \quad dom \quad x) \end{array}$$

Pareto front. The set of all Pareto-optimal solutions is called a Pareto front $\mathcal{F}$. Inside the front, no solution dominates another.

$$\begin{array}{ccc} x \in \mathcal{F} & \Longleftrightarrow & \forall \quad y \in \mathcal{F}, \\ \neg(y \quad dom \quad x) & \wedge & \neg(x \quad dom \quad y) \end{array}$$

A. Method 1: an aggregative approach, the weighted sum

This method $\mathcal{M}_1$ is a mono-objective optimization method based on the representation of all the objectives f_i by a single cost function f to minimize, expressed as a weighted sum of all individual f_i and their corresponding weighting factors w_i as in the following equation:

$$f = \sum_{i=1}^{n} w_i . f_i(\mathbf{x}), \quad \mathbf{x} \in \mathbb{R}^N \tag{1}$$

where: $0 < w_i < 1$ and $\Sigma w_i = 1$ *(weights condition)*. After that, a classical mono-criteria optimization technique is applied, such as in our case the *Nelder-Mead* method [15], to find an optimum. This method is straight-forward and can always find a solution, but may prematurely converge to a local optimum. This problem can be overcome, for instance by using an initialization phase to start the optimization process close to a known optimum, or close to j different optima to obtain j most optimal solutions, as explained for instance in [11].

By varying weights w_i, different entry points minimizing the global objective function f can be obtained. By trying all, or a high number of different combinations of parameters w_i, we can obtain all the possible optimal entry points that can be found with this method, using an approach derived from [10]. So far, we constitute a stochastic uniform sampling of the weights parameters in such a way that for n objective function f_i, a sample contains nw_i conforming to the mentioned *weights condition*. A *Dirichlet* distribution [16] (see Fig. 2) allows to obtain a uniform sampling of the parameters.

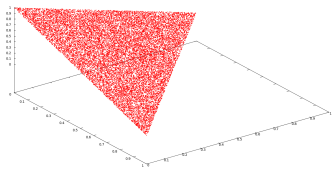

Fig. 2: Uniform sampling of combinations of w_i using a *Dirichlet* distribution

Let us denote $\mathcal{S}_1$ the set of optimal points corresponding to all tested weights combinations. Its first Pareto front $\mathcal{S}_1\mathcal{F}_1 \subset \mathcal{S}_1$, *i.e.* the points of $\mathcal{S}_1$ that are not dominated by any other, can be extracted from $\mathcal{S}_1$, and compared with the Pareto fronts of the two other methods.

B. Method 2: a well known evolutionary approach: NSGA-II

Method $\mathcal{M}_2$ is a evolutionary multi-objective optimization method based on a Pareto ranking scheme. The Non-dominated Sorting Genetic Algorithm II (NSGA-II) [7] has been chosen as it is well suited for multi-objective continuous problems, with a complexity of $O(mn^2)$, where m is the number of objectives and n the population's size, making it usable in a reasonable time for our kind of application. If n is really large, other algorithms such as ASREA or G-ASREA

[22], [23] have been devised that have an $O(man)$ complexity (where a is an archive of size $10m$) and that can be massively parallelized.

1) NSGA-II principle: the algorithm consists in two phases:

1. *initialization phase:* an initial population $\mathcal{P}_0$ of size N is selected randomly from the initial solution space $\mathcal{S}$. A first offspring generation $\mathcal{Q}_0$ of size N is then created by a tournament selection on $\mathcal{P}_0$ over the values of the m objective functions f_i, followed by crossover and mutation processes.

2. *iterative phase:* the population is evolved until reaching a certain number of generations. For the t^{th} generation, a combined population $\mathcal{R}_t$ of size $2N$ is formed from the current population $\mathcal{P}_t$ and the offspring generation $\mathcal{Q}_t$. Since all the previous and current best individuals are added in the population, elitism is ensured. $\mathcal{R}_t$ is then sorted based on non-dominance and crowding-comparison approach which guides the selection process at the various stages of the algorithm toward a uniformly spread-out Pareto optimal front thanks to a density-estimation metrics without need of a sharing parameter. The new generation $\mathcal{P}_{t+1}$ is filled by each front subsequently until the population size exceeds N. If by adding all the individuals in front $\mathcal{F}_j$ the population exceeds N then individuals in front $\mathcal{F}_j$ are selected based on their crowding distance in the descending order until the population size becomes equal to N. The process is repeated until the desired offspring generation is reached. Then the last population becomes the set $\mathcal{S}_2$ of optimal points from method $\mathcal{M}_2$. See [7] for a complete description of the algorithm.

2) NSGA-II setup: an initialization is done with a population size equals to 2000. Individuals are initialized randomly over the surface of the solution space (Fig. 3a); and the algorithm has been run run over 10 generations. After that, a *DBX* Dominance Based Restricted selection [17] has been used to choose the offspring individuals, followed by a blend alpha recombination (BLX-α) [9] for the *crossover function*. In BLX-α, an offspring c is generated by a random linear recombination of the parents $p1$ and $p2$ as follows: $c_k = (1-\gamma_i)p_{1,k} + \gamma_i p_{2,k}$ where $\gamma_i = (1+2\alpha)u_i - \alpha$ with u_i a random number between 0 and 1, and $\alpha = 0.5$ in our experiments. The crossover probability has been set to 0.9, with a crossover distribution index $eta_c = 10$. A *polynomial mutation function* has been chosen for a child c_k and a parent p_k as follows: $c_k = p_k + (p_k^u - p_k^l)\delta_k$ with p_k^u, p_k^l the upper and lower bounds for the parents, while δ_k is a small random variation calculated via a polynomial distribution. The mutation rate has been set to 0.5, with a mutation distribution index eta_m equals to 5. Finally, the *evaluation* is performed for the three objective functions described in IV-C.

C. Method 3: quasi-exhaustive dominance-based method

The third method $\mathcal{M}_3$, based on a Monte-Carlo approach, is considered as a ground truth for our experiments. It consists in analyzing the dominance on a very large distribution of randomly sampled points in the solution space. Let us denote $\mathcal{S}_3$ the set of samples. We compute the Pareto front $\mathcal{S}_3\mathcal{F}_1 \subset \mathcal{S}_3$ according to the dominance rule described above. Fig. 3b shows the dense sampling of the initial solution space. This method has long computation times, making it unsuitable for a clinical use despite its wide and extensive coverage of the space of candidate entry points.

IV. Description of the experiment

In this section we describe the experimental setup, tests pipelines, and measures. Then we explain the use case and the datasets on which tests in this study have been performed. At last we illustrate quantitative information on charts, with an illustrative snapshots and comments.

A. Experimental pipeline

The objective of the test was to compare the three methods on their coverage over the surface of candidate entry points, and their ability to find the maximal set of optimal solutions.

To this end, we have implemented a pipeline illustrated in Fig. 4. Starting from the initial space of candidate entry points $\mathcal{S}$, it proceeds as follows:

Step 1: "Optimal sets".

We compute $\mathcal{S}_1$ containing the 60.000 best solutions obtained when running Nelder-Mead optimization $\mathcal{M}_1$. with $j = 3$ for 20.000 times on different random combination of weights. We compute $\mathcal{S}_2$ in $\mathcal{M}_2$ using NSGA-II according to the settings described in III-B2. Finally we compute $\mathcal{S}_3$ containing a sample of 100.000 random entry points with the quasi-exhaustive search method $\mathcal{M}_3$.

Step 2: "Pareto fronts".

For $\mathcal{S}_1$, $\mathcal{S}_2$, and $\mathcal{S}_3$, we compute the first Pareto fronts, respectively named $\mathcal{S}_1\mathcal{F}_1$, $\mathcal{S}_2\mathcal{F}_1$, and $\mathcal{S}_3\mathcal{F}_1$, according to the dominance rule. These sets contain the non-dominated solutions from their source sets.

Step 3: "Non-dominance test".

In this step, we filter $\mathcal{S}_1\mathcal{F}_1$, $\mathcal{S}_2\mathcal{F}_1$, and $\mathcal{S}_3\mathcal{F}_1$ by eliminating the points that are dominated by points found by another method using a non-dominance (ND) test. By filtering front $\mathcal{S}_i\mathcal{F}_1$ with points of front $\mathcal{S}_j\mathcal{F}_1$, we obtain the set $\mathbf{ND}_{ij}$ of points of $\mathcal{S}_i\mathcal{F}_1$ that are not dominated by points of $\mathcal{S}_j\mathcal{F}_1$. In the rest of the paper, we will call these points *elite points* of $\mathcal{S}_i\mathcal{F}_1$. The results are six subsets named *NDsets*: $\{\mathbf{ND}_{12}, \mathbf{ND}_{13}\} \subset \mathcal{S}_1\mathcal{F}1$, $\{\mathbf{ND}_{21}, \mathbf{ND}_{23}\} \subset \mathcal{S}_2\mathcal{F}1$, and $\{\mathbf{ND}_{31}, \mathbf{ND}_{32}\} \subset \mathcal{S}_3\mathcal{F}1$.

Step 4: "Distance filter".

Finally, we noticed that the $\mathbf{ND}_{ij}$ sets may contain solutions which are very close in terms of locations (and therefore evaluations). Thus, we added another filter keeping only the distinct solutions, using an Euclidean distance metric. The result of the filter is six subsets named *NDCsets* $\mathbf{NDNC}_{ij} \subset \mathbf{ND}_{ij}$, with $\mathbf{NDNC}_{ij}$ containing points from $\mathcal{S}_i\mathcal{F}1$ that are not dominated by any point of $\mathcal{S}_j\mathcal{F}1$ and that are not located close to a point of $\mathcal{S}_j\mathcal{F}1$(NDNC for Not Dominated Not Close). In other words, $\mathbf{NDNC}_{ij}$ covers areas containing elite points found by method $\mathcal{M}_i$ but no elite points found by method $\mathcal{M}_j$. After that the closest points have been clustered in order to highlight the areas of the surface of candidate points where elite points have been found by one method and not by another.

(a) $\mathcal{S}2$ (b) $\mathcal{S}3$

Fig. 3: Initial samplings for methods $\mathcal{M}_2$ and $\mathcal{M}_3$

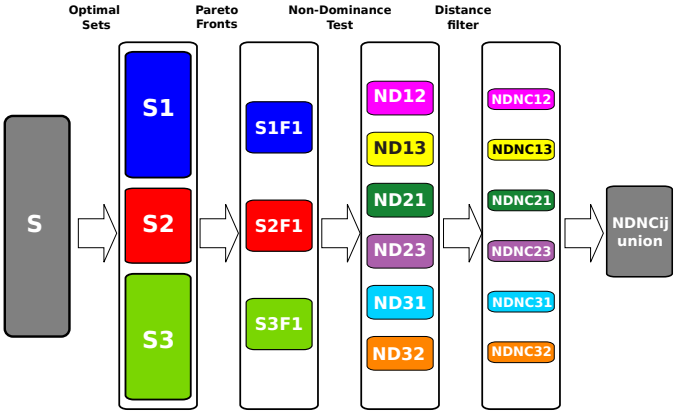

Fig. 4: Sets pipeline

B. Comparison of the three methods

The number of points in the Pareto fronts is not a good indicator of the ability of a method to discover points where other methods couldn't, as it also strongly depends on the location of the points and their density. We have chosen to compare the coverage areas instead of the number of points.

We have first subdivided the triangular mesh representing the surface of possible candidate entry points on the skin. The level of subdivision has been chosen empirically. The triangles need to be not too small otherwise they would be reduced to the size of a single point and we have no benefit of using surfaces instead of points, and not too large otherwise the precision would be too low. The average size of a triangle has been set to a maximum of 1 mm^2.

For each set, we have located all the triangles containing at least one of its points, and created a surface as the aggregation of all the triangles. The areas of the created surfaces have been computed.

C. Use-case and experimental data

To test and compare the three methods on the trajectory planning procedure of a minimally invasive surgery, we have chosen to use data of patients who underwent Deep Brain Stimulation electrodes implantation. Deep Brain Stimulation is a neurosurgical procedure intended to treat motion disorders such as Parkinson's disease. It consists in implanting permanent electrodes in deep structures of the brain, and to continuously stimulate them. The electrode trajectory planning is submitted to a number of surgical rules, among which we have chosen to study three of them as objective functions for our experiment, that are described in more detail in [10].

- "ST": Orientation of the electrode, computed as the proximity to a standard trajectory (ST) defined by expert neurosurgeons and commonly used in the commercial platforms.
$$f_{ST} = \frac{angle(T,ST)}{90}$$
- "DS": Distance from the electrode to vessels, computed as the distance to the closest sulci.
$$f_{D_S} = Max(\frac{D_{minS} - dist(T,S)}{D_{minS}}, 0)$$
- "DV": Distance from the electrode to ventricles.
$$f_{D_V} = Max(\frac{D_{minV} - dist(T,V)}{D_{minV}}, 0)$$

An illustration of these constraints is shown on Fig. 5.

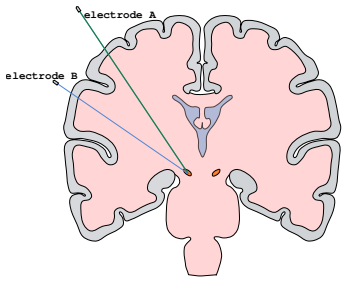

Fig. 5: The structures of interest inside the brain: the target is the small lense shape sturcture in orange, ventricles in blue, and vessels embedded in the sulci in gray. Two candidate electrode trajectories are illustrated: electrode A satisfies the constraint "ST" better than electrode B, while electrode B satisfies "DV" better than electrode A.

The tests have been performed on 30 retrospective datasets of preoperative images of 15 patients issued from 2 different hospitals, and who underwent bilateral DBS implant. All were treated for Parkinson's disease, and the target was the Subthalamic Nucleus. The images consisted in 3T T1-weighted MRI (1.0mm x 1.0mm x 1.0mm, Philips Medical Systems) for Hospital 1, and 1.5T T1-weighted MRI (0.9373mm x 0.9375mm x 1.3mm, GE Medical systems) for Hospital 2. The 3D brain model has been reconstructed using pyDBS [5] pipeline. A model consists of triangular surface meshes of the sulci, the ventricles, the subthalamic nucleus, and a skin patch representing the initial solution space $\mathcal{S}$. Experiments have been performed on an Intel Core i7 running at 2.67 GHz with 8GB RAM workstation.

V. Results and discussion

The obtained results from the 30 cases are summarized in the three charts of Fig. 10, 11, and 12, and illustrate the quantitative information of the solution surfaces areas, while the visual information of the insertion points location and their coverage surfaces are illustrated by snapshots (Figs. 6 to 9) on a single case #26.

Fig. 10 shows the areas covered by the Pareto fronts for each of the three methods. As expected, the surfaces covered by the reference method $\mathcal{M}_3$ are the largest. Among the two optimization methods, $\mathcal{M}_2$ provides the largest coverage with a mean of 85.23 mm^2 compared to 51.75 mm^2 for $\mathcal{M}_1$. In Fig. 6 the three fronts are superimposed over the initial solution space mesh (the zone of the scalp corresponding to feasible entry points). It can be noticed that the solutions of $\mathcal{M}_1$ and $\mathcal{M}_2$ are different, and they are more or less contained in the solutions of $\mathcal{M}_3$. A zoom on the area of interest is shown in Fig. 7 for each of the fronts separately. On Figs. 8a and 8b, the solutions of $\mathcal{M}_1\mathcal{F}_1$ and $\mathcal{M}_2\mathcal{F}_1$ are superimposed on the solutions of $\mathcal{M}_3\mathcal{F}_1$, allowing to compare visually the coverage of $\mathcal{M}_1$ and $\mathcal{M}_2$ compared to method $\mathcal{M}_3$.

We can see in Fig. 11 the areas of the non-dominated solution sets $\mathbf{ND}_{ij}$ surfaces for two methods at a time. It can be noticed that the areas of solutions detected by $\mathcal{M}_1$ and $\mathcal{M}_2$ which are not dominated by solutions in $\mathcal{M}_3$ are relatively small (see $\mathbf{ND}_{13}$ and $\mathbf{ND}_{23}$) since that $\mathcal{M}_3$ is a quasi-exhaustive method and supposed to detect the maximum number of solutions. Despite that, both $\mathcal{M}_1$ and $\mathcal{M}_2$ are able to find a few solutions more interesting than $\mathcal{M}_3$ thanks to the efficiency of optimization. When comparing $\mathcal{M}_1$ and $\mathcal{M}_2$, we can observe that both methods could find elite points not discovered by the other (see $\mathbf{ND}_{12}$ and $\mathbf{ND}_{21}$, both on Fig. 11 and Table I), with a small advantage for method $\mathcal{M}_2$. This can also be observed on the snapshot of Fig.9a that displays the coverage of $\mathbf{ND}_{12}$ over $\mathbf{ND}_{21}$.

The non-dominated non-close solutions sets (NDNC sets) allow to highlight areas where some methods can propose solutions and others do not. The large areas missed by methods $\mathcal{M}_1$ and $\mathcal{M}_2$ can be visualize in Fig. 9b.

The most remarkable information is that the areas of elite points found by $\mathcal{M}_3$ and not by $\mathcal{M}_1$ (corresponding to $\mathbf{ND}_{31}$ in Fig. 11) are very large, which emphasizes the fact that the mono-objective weighted sum approach can miss a large number of interesting solutions. The zones detected by $\mathcal{M}_3$ and not by $\mathcal{M}_2$ are smaller ($\mathbf{ND}_{32}$ in Fig. 11) since that $\mathcal{M}_2$ and $\mathcal{M}_3$ have close concepts. Table I summarizes coverage for the comparison between $\mathcal{M}_1$ and $\mathcal{M}_2$.

TABLE I: Mean coverage of the solution space by methods 1 and 2 compared to each other and to method 3

	$\mathcal{S}_1\mathcal{F}_1$		$\mathcal{S}_2\mathcal{F}_1$		$\mathbf{ND}_{12}$	$\mathbf{ND}_{21}$	$\mathbf{NDNC}_{12}$	$\mathbf{NDNC}_{21}$
	area	% of $\mathcal{S}_3\mathcal{F}_1$	area	% of $\mathcal{S}_3\mathcal{F}_1$				
AVG	51.75	28.35	85.23	44.96	51.68	84.79	6.84	32.53
STD	15.02	6.67	30.06	8.02	15.01	29.82	3.40	19.57

Another important information is that none of the experimented methods were able to find the totality of the solutions. Significant areas are found by each of the methods and not by the others. This is due to several factors. The quasi-exhaustive method does not optimize the solutions and is dependent on the random sorting, which make that it can miss good solutions. The results of the weighted sum confirm the well-know drawbacks of this method, that leads to an inhomogeneous distribution of the solutions over the Pareto front. Evolutionary method $\mathcal{M}_2$ is a compromise between fast computation time and number of tested points, and a better coverage of the area would be at the price of a higher number of points and longer computations.

The computation times are about 20 mn for method $\mathcal{M}_1$, about 30 sec. for $\mathcal{M}_2$, and 5 mn for method $\mathcal{M}_3$. Even if $\mathcal{M}_3$ is the one providing the best coverage, it is not usable in a reasonable time compatible with clinical routine, whereas method $\mathcal{M}_1$ can provide a single updatable result in a few seconds. This is why we think that hybrid methods for optimization or for display in GUI, or extensions of weighted sum method [13] should be investigated.

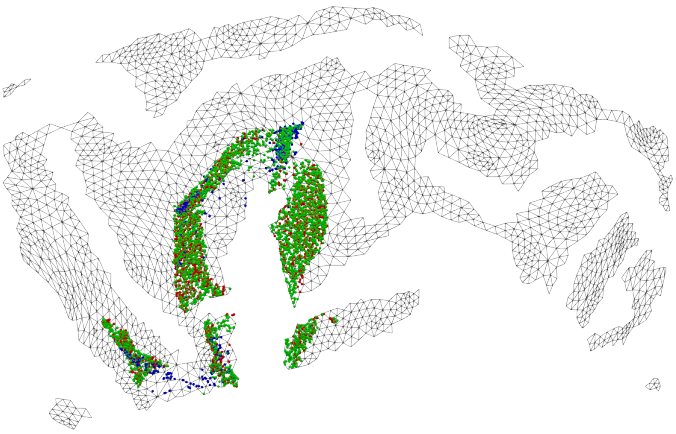

Fig. 6: Overview of the surface of possible entry points, with the three Pareto fronts: $\mathcal{S}_1\mathcal{F}_1$ in blue, $\mathcal{S}_2\mathcal{F}_1$ in red, $\mathcal{S}_1\mathcal{F}_1$ in green

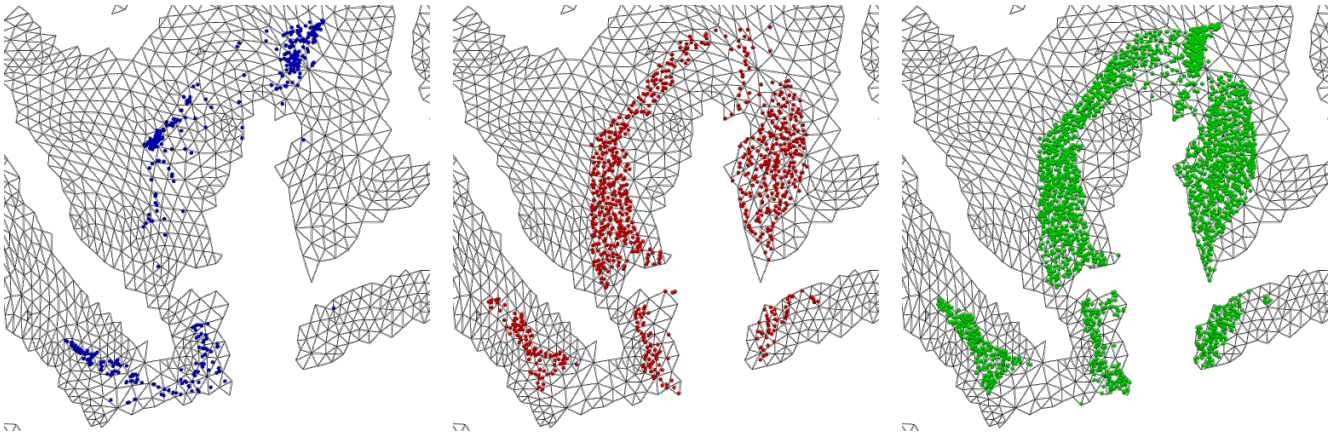

(a) $\mathcal{S}_1\mathcal{F}_1$ (b) $\mathcal{S}_2\mathcal{F}_1$ (c) $\mathcal{S}_3\mathcal{F}_1$

Fig. 7: Zoom on the Pareto fronts of $\mathcal{M}_1$ in blue, $\mathcal{M}_2$ in red, and $\mathcal{M}_3$ in green

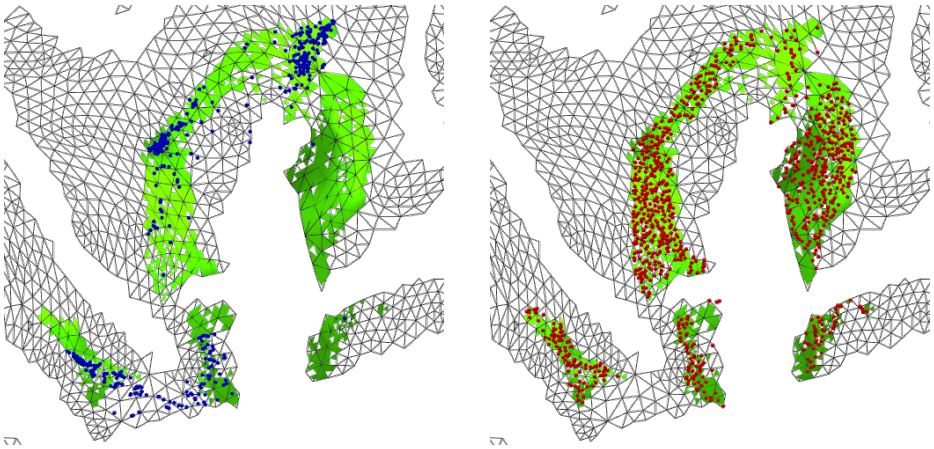

(a) $\mathcal{S}_1\mathcal{F}_1$ points over $\mathcal{S}_3\mathcal{F}_1$ surface (b) $\mathcal{S}_2\mathcal{F}_1$ points over $\mathcal{S}_3\mathcal{F}_1$ surface

Fig. 8: Coverage of methods $\mathcal{M}_1$ and $\mathcal{M}_2$ compared to $\mathcal{M}_3$

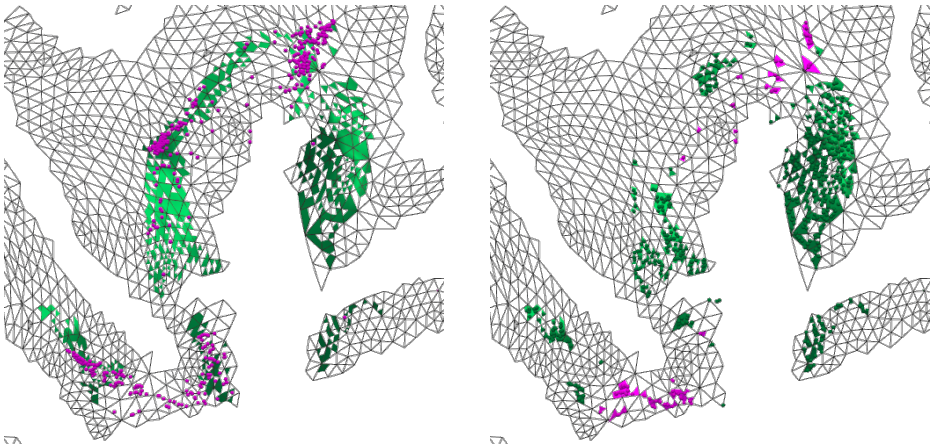

(a) $\mathbf{ND}_{12}$ points over $\mathbf{ND}_{21}$ surface (b) $\mathbf{NDC}_{12}$ and $\mathbf{NDC}_{21}$

Fig. 9: Comparison between coverage by elite points of methods $\mathcal{M}_1$ and $\mathcal{M}_2$

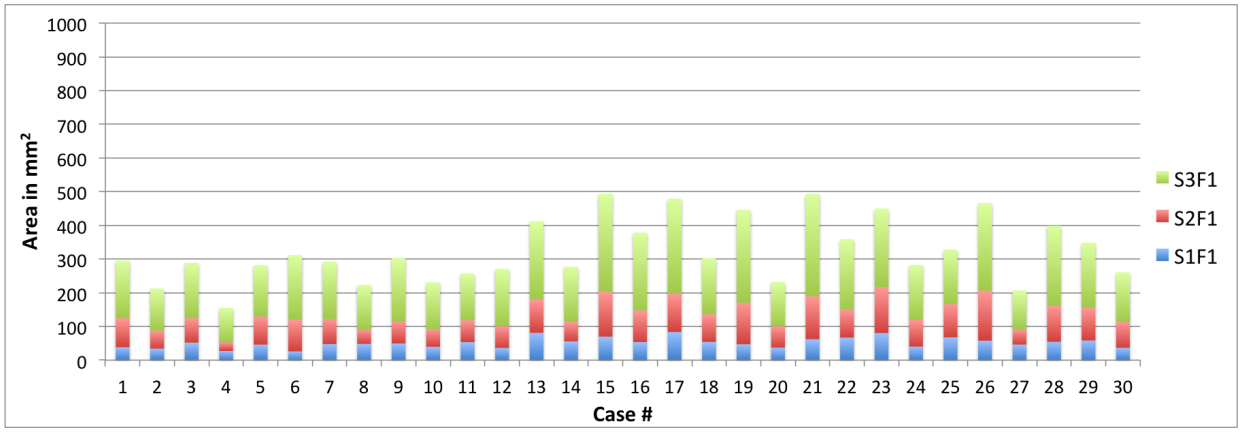

Fig. 10: Surfaces areas of the Pareto fronts in the three methods

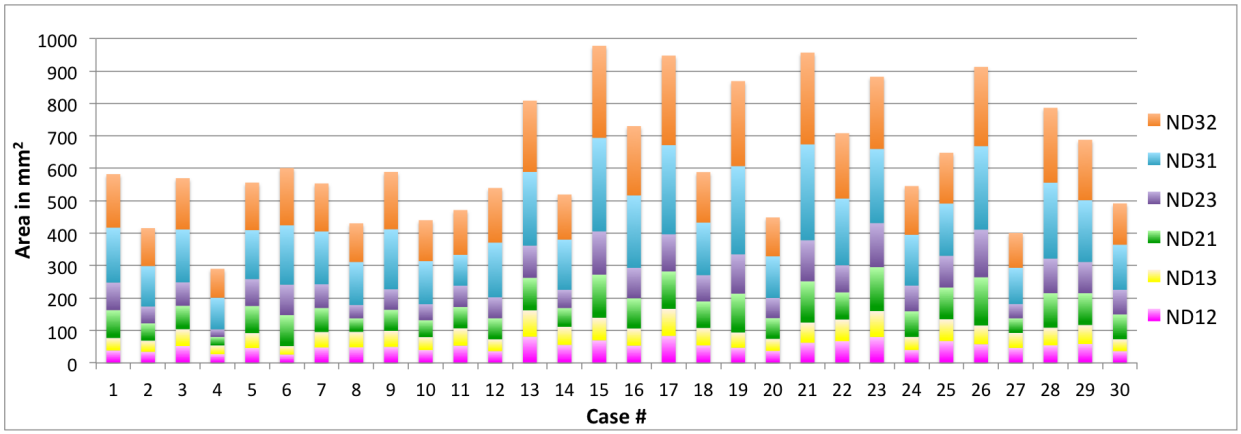

Fig. 11: The six non-dominated sets for each of the 30 datasets

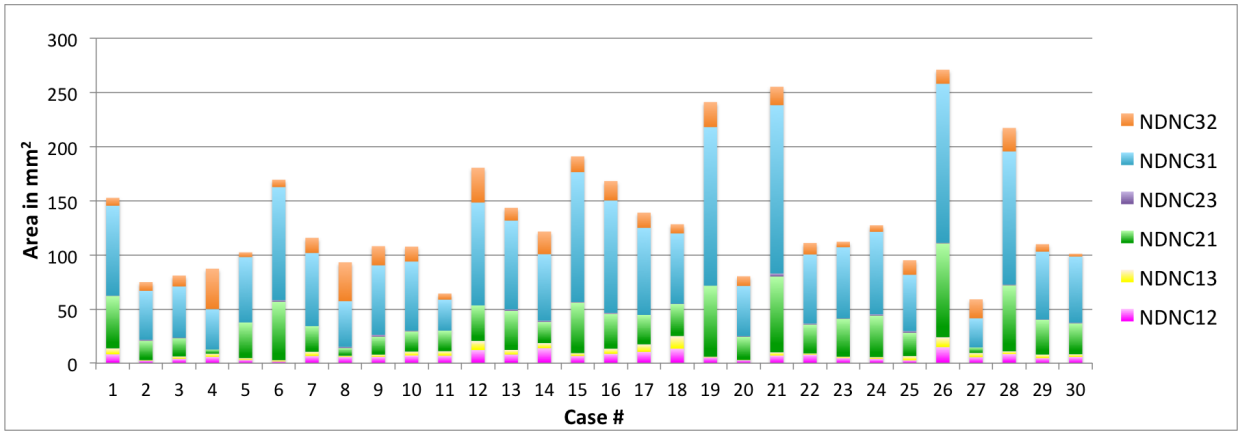

Fig. 12: The six non-dominanated not-close sets for each of the 30 datasets

VI. Discussion and Conclusions

In surgical planning, most of the automatic trajectory planning techniques that have been proposed in the literature are based on mono-objective optimization approaches that combine different criteria through weighted sums. Unfortunately, theory shows that such techniques cannot find concavities in Pareto-fronts, meaning that some Pareto-optimal solutions cannot be found. Based on experimental results on 30 real patient-specific data, this paper shows that in practice, basic Pareto based optimization methods such as NSGA-II can indeed find more optimal solutions than the current state of the art in weighted sums optimization algorithms, and hence extending the range of the optimal solutions to surgeons. NSGA-II was tested first because it is one of the most versatile multi-objective dominance based algorithms. It can therefore serve as a basis to explore the potential of such optimization algorithms.

Future work will now consist in developing tailored algorithms that will specialize on the specific problem of automatic trajectory planning techniques. Finally, hybrid visualization of the solutions in the GUI can also be enhanced to simplify the surgeon task.

References

[1] C. Baegert, C. Villard, P. Schreck, and L. Soler. Multi-criteria trajectory planning for hepatic radiofrequency ablation. In *proceedings of MICCAI'07*, volume 4791 of *Springer LNCS*, pages 584–592, 2007.

[2] S. Bériault, F. A. Subaie, D. L. Collins, A. F. Sadikot, and G. B. Pike. A multi-modal approach to computer-assisted deep brain stimulation trajectory planning. *Int J CARS*, 7(5):687–704, jun 2012.

[3] E. Brunenberg, A. Vilanova, V. Visser-Vandewalle, Y. Temel, L. Ackermans, B. Platel, and B. ter Haar Romeny. Automatic trajectory planning for deep brain stimulation: A feasibility study. In *proceedings of MICCAI'07*, volume 4791 of *Springer LNCS*, pages 584–592, 2007.

[4] D. Craft. Multi-criteria optimization methods in radiation therapy planning: a review of technologies and directions. *arXiv preprint arXiv:1305.1546*, 2013.

[5] T. D'Albis, C. Haegelen, C. Essert, S. Fernandez-Vidal, F. Lalys, and P. Jannin. PyDBS: an automated image processing workflow for deep brain stimulation surgery. *International Journal of Computer Assisted Radiology and Surgery*, pages 1–12, 2014.

[6] I. Das and J. Dennis. A closer look at drawbacks of minimizing weighted sums of objectives for pareto set generation in multicriteria optimization problems. *Structural optimization*, 14(1):63–69, 1997.

[7] K. Deb, A. Pratap, S. Agarwal, and T. Meyarivan. A fast and elitist multiobjective genetic algorithm: Nsga-ii. *Evolutionary Computation, IEEE Transactions on*, 6(2):182–197, 2002.

[8] P.-F. D'Haese, S. Pallavaram, R. Li, M. S. Remple, C. Kao, J. S. Neimat, P. E. Konrad, and B. M. Dawant. Cranialvault and its crave tools: A clinical computer assistance system for deep brain stimulation (DBS) therapy. *Medical Image Analysis*, 16(3):744 – 753, 2012.

[9] S. J. Eshelman, Larry J. *Real-Coded Genetic Algorithms and Interval-Schemata*. 1993.

[10] C. Essert, S. Fernandez-Vidal, A. Capobianco, C. Haegelen, C. Karachi, E. Bardinet, M. Marchal, and P. Jannin. Statistical study of parameters for deep brain stimulation automatic preoperative planning of electrodes trajectories. *International journal of computer assisted radiology and surgery*, pages 1–11, 2015.

[11] C. Essert, C. Haegelen, F. Lalys, A. Abadie, and P. Jannin. Automatic computation of electrode trajectories for deep brain stimulation: a hybrid symbolic and numerical approach. *International journal of computer assisted radiology and surgery*, 7(4):517–532, 2012.

[12] N. Hamze, J. Voirin, P. Collet, P. Jannin, C. Haegelen, and C. Essert. Pareto front vs. weighted sum for automatic trajectory planning of deep brain stimulation. In *Medical Image Computing and Computer Assisted Intervention (MICCAI'16)*, volume 9900 of *LNCS*, pages 534–541. Springer, Oct 2016. (CORE rank A).

[13] I. Kim and O. de Weck. Adaptive weighted sum method for multiobjective optimization: a new method for pareto front generation. *Structural and Multidisciplinary Optimization*, 31(2):105–116, 2006.

[14] J. Koski. Defectiveness of weighting method in multicriterion optimization of structures. *Communications in Applied Numerical Methods*, 1(6):333–337, 1985.

[15] J. Nelder and R. Mead. A simplex method for function minimization. *Computer Journal*, 7(4):308–313, 1965.

[16] K. W. Ng, G.-L. Tian, and M.-L. Tang. *Dirichlet and related distributions: Theory, methods and applications*, volume 888. John Wiley & Sons, 2011.

[17] O. Rudenko and M. Schoenauer. Dominance based crossover operator for evolutionary multi-objective algorithms. In X. Yao, E. Burke, J. Lozano, J. Smith, J. Merelo-Guervs, J. Bullinaria, J. Rowe, P. Tio, A. Kabn, and H.-P. Schwefel, editors, *Parallel Problem Solving from Nature - PPSN VIII*, volume 3242 of *Lecture Notes in Computer Science*, pages 812–821. Springer Berlin Heidelberg, 2004.

[18] C. Schumann, J. Bieberstein, C. Trumm, D. Schmidt, P. Bruners, M. Niethammer, R. T. Hoffmann, A. H. Mahnken, P. L. Pereira, and H.-O. Peitgen. Fast automatic path proposal computation for hepatic needle placement. In *SPIE Medical Imaging*, pages 76251J–76251J. International Society for Optics and Photonics, 2010.

[19] C. Schumann, C. Rieder, S. Haase, K. Teichert, P. Süss, P. Isfort, P. Bruners, and T. Preusser. Interactive multi-criteria planning for radiofrequency ablation. *Int J CARS*, apr 2015.

[20] A. Seitel, M. Engel, C. Sommer, B. Redeleff, C. Essert-Villard, C. Baegert, M. Fangerau, K. Fritzsche, K. Yung, H.-P. Meinzer, and L. Maier-Hein. Computer-assisted trajectory planning for percutaneous needle insertions. *Medical Physics*, 38(6):3246–3260, 2011.

[21] R. Shamir, I. Tamir, E. Dabool, L. Joskowicz, and Y. Shoshan. A method for planning safe trajectories in image-guided keyhole neurosurgery. In *proceedings of MICCAI'10*, volume 6363, pages 457–464. Springer LNCS, 2010.

[22] D. Sharma and P. Collet. An archived-based stochastic ranking evolutionary algorithm (ASREA) for multi-objective optimization. In *GECCO '10: Proceedings of the 12th annual conference on Genetic and evolutionary computation*, pages 479–486, New York, NY, USA, 2010. ACM.

[23] D. Sharma and P. Collet. Gpgpu-compatible archive based stochastic ranking evolutionary algorithm (g-asrea) for multi-objective optimization. In *PPSN (2)*, pages 111–120, 2010.